Berliner, L. J. (1978) *Methods Enzymol. 49G*, 418-480.
De Boeck, H., Loontiens, F. G., Delmotte, F. M., & De Bruyne, C. K. (1981) *FEBS Lett. 126*, 227-230.
Delmotte, F. M., & Goldstein, I. J. (1980) *Eur. J. Biochem. 112*, 219-223.
Goldstein, I. J., Blake, D. A., Ebisu, S., Williams, T. J., & Murphy, L. A. (1981) *J. Biol. Chem. 256*, 3890-3893.
Murakami, K., Andree, P. J., & Berliner, L. J. (1982) *Biochemistry 21*, 5488-5494.
Murphy, L. A., & Goldstein, I. J. (1977) *J. Biol. Chem. 252*, 4739-4742.
Murphy, L. A., & Goldstein, I. J. (1979) *Biochemistry 18*, 4999-5005.
Plessas, N. R., & Goldstein, I. J. (1981) *Carbohydr. Res. 89*, 211-220.
Poulsen, F. M., Johansen, J. T., & Pedersen, J. A. (1977) *Carlsberg Res. Commun. 42*, 368-378.
Rackwitz, H.-R. (1981) *Carbohydr. Res. 88*, 223-232.
Struve, W. G., & McConnell, H. M. (1972) *Biochem. Biophys. Res. Commun. 49*, 1631-1637.
Suzuki, T., Inoue, K., Nojima, S., & Wiegandt, H. (1983) *J. Biochem. (Tokyo) 94*, 373-377.
Wien, R. W., Morrisett, J. D., & McConnell, H. M. (1972) *Biochemistry 11*, 3707-3716.
Wood, C., Kabat, E. A., Murphy, L. A., & Goldstein, I. J. (1979) *Arch. Biochem. Biophys. 198*, 1-11.

Articles

Wheat Germ Agglutinin Dimers Bind Sialyloligosaccharides at Four Sites in Solution: Proton Nuclear Magnetic Resonance Temperature Studies at 360 MHz†

K. Anne Kronis‡ and Jeremy P. Carver*

Departments of Medical Genetics and Medical Biophysics, University of Toronto, Toronto, Ontario, Canada M5S 1A8
Received May 2, 1984; Revised Manuscript Received August 28, 1984

ABSTRACT: Equilibrium binding studies have been performed over a range of temperatures from 25.4 to 47.3 °C between wheat germ agglutinin isolectin I (WGA I) and the α2-3 isomer of (*N*-acetylneuraminyl)lactose (NeuNAcα2-3Galβ1-4Glc). Proton nuclear magnetic resonance spectroscopy at 360 MHz has been used to monitor titrations in this system under conditions where the fraction of total ligand which is bound is small, yet the fractional occupation of sites covers a wide range. Several of the ligand resonances, including the *N*-acetyl methyl and the axial and equatorial hydrogens at carbon 3 of the NeuNAc residue, are shifted and broadened in the presence of WGA due to chemical exchange between the free and bound environments. The lifetime broadening of the *N*-acetyl resonance at room temperature of a series of related sialyloligosaccharides has been previously used by us to measure binding affinities to two WGA isolectins [Kronis, K. A., & Carver, J. P. (1982) *Biochemistry 21*, 3050-3057]. In this paper we report the temperature dependence of the apparent bound shifts and the apparent bound line widths of the *N*-acetyl, H3a, and H3e peaks. The true bound shifts for the three resonances have been obtained from these data by using the equations derived by Swift and Connick [Swift, T. J., & Connick, R. E. (1962) *J. Chem. Phys. 37*, 307-320]. The total bound shifts, per monomer, were found to be -1.98, -4.0, and -0.8 ppm for the *N*-acetyl, the H3a, and the H3e resonances, respectively. The *N*-acetyl data are consistent with there being four NeuNAc binding sites on the WGA I dimer, each with a bound shift for the *N*-acetyl resonance of -0.99 ± 0.03 ppm. This is in contrast to the X-ray diffraction studies that revealed only two NeuNAc sites per dimer. The sources of the ring current shifts for the *N*-acetyl resonance have been assigned to two equivalent sets of tyrosine aromatic side chains per monomer (Tyr-73 and Tyr-159). When the ^{1}H NMR and the X-ray diffraction data are compared, it is apparent that the bound NeuNAc residue occupies a position in each binding site that is analogous to that occupied by the terminal GlcNAc of WGA-bound oligomers of GlcNAc. The *N*-acetyl of the bound NeuNAc or GlcNAc residue is oriented in the same way over the face of a Tyr ring in each binding site.

Wheat germ agglutinin (WGA)[1] is one of the more widely used of the plant lectins in probing the carbohydrate moieties of cell surfaces and mammalian tissues. The sugar specificity of a lectin such as WGA is generally defined on the basis of

† This research was supported by grants from the National Cancer Institute of Canada and from the Medical Research Council of Canada (MT-3732 and MA-6499). This paper represents part of the Ph.D. thesis work of K.A.K.

* Address correspondence to this author at the Department of Medical Genetics.

‡ Present address: Departments of Chemistry and Biology, Massachusetts Institute of Technology, Cambridge, MA 02139.

[1] Abbreviations: WGA, wheat germ agglutinin; NeuNAc, *N*-acetyl-D-neuraminic acid; N3L, NeuNAcα2-3Galβ1-4Glc; ^{1}H NMR, proton nuclear magnetic resonance; GlcNAc, *N*-acetyl-D-glucosamine; $(GlcNAc)_2$, GlcNAcβ1-4GlcNAc; $(GlcNAc)_3$, GlcNAcβ1-4GlcNAcβ1-4GlcNAc; $(GlcNAc)_2\beta$1-Me, GlcNAcβ1-4GlcNAcβ1-CH_3; N3Ln, NeuNAcα2-3Galβ1-4GlcNAc; DSS, sodium 4,4-dimethyl-4-silapentane-1-sulfonate; NAc, *N*-acetyl; Me, methyl; CD, circular dichroism.

0006-2960/85/0424-0826$01.50/0

the monosaccharide or small oligosaccharides which are the most potent inhibitors of lectin-mediated processes such as agglutination of cells or precipitation of glycoconjugates (Goldstein et al., 1980). Of the commonly occurring sugars, *N*-acetylglucosamine (GlcNAc) and its β1–4 linked oligomers are the best inhibitors of WGA [for a review, see Goldstein & Hayes (1978)]. Traditionally, the specificity of WGA has been defined as being for these sugars. However, much of the experimental use of WGA involves its binding to mammalian cells and tissues. In these studies, it has repeatedly been found that *N*-acetylneuraminic acid (NeuNAc) residues play a central role (Burger & Goldberg, 1967; Cuatrecasas, 1973; Adair & Kornfeld, 1974; Stanley & Carver, 1977; Stanley et al., 1980). Hence, it is essential to understand the molecular features of WGA–NeuNAc interactions, if WGA is to be useful as a probe of mammalian sugar structures.

In a previous study at 24 °C, we examined the affinities of WGA I and WGA II isolectins for a series of NeuNAc-terminating trisaccharides by quantifying the lectin-induced lifetime broadening of the *N*-acetyl resonance of the ligand in the proton nuclear magnetic resonance (^{1}H NMR) spectra at 360 MHz (Kronis & Carver, 1982). The data were interpreted as indicating that an aromatic amino acid side chain was in close proximity to the *N*-acetyl methyl group of these ligands. In addition, a higher affinity was found for the α2–3 linkage form of a NeuNAc-terminating oligosaccharide when compared with the α2–6 isomer. Earlier estimates of the number of NeuNAc binding sites per dimer have ranged from 2 to 12 (Greenaway & LeVine, 1972; Jordan et al., 1977; Peters et al., 1979; Bhavanandan & Katlic, 1979). In addition, the aromatic amino acid responsible for shifting the *N*-acetyl resonance of NeuNAc and GlcNAc was postulated by Jordan et al. (1977) to be tryptophan. In this paper we report that there are four binding sites on the WGA dimer for NeuNAcα2–3Galβ1–4Glc, identify the aromatic amino acid side chain near the *N*-acetyl methyl group in each site as being a tyrosine, and compare the data with those previously obtained for GlcNAc-terminating oligosaccharides. The results presented below agree with the NeuNAc–WGA crystal complexes (Wright, 1980a,b) with regard to the involvement of tyrosines and the orientation of the *N*-acetyl group. However, in solution four binding sites have been found per dimer whereas only two were detected in the X-ray studies.

Experimental Procedures

Materials. WGA I was isolated as described in Kronis & Carver (1982) by affinity purification of the mixture of isolectins on an ovomucoid–Sepharose 4B column (Marchesi, 1972) and subsequent separation of the isolectins on CM-Sepharose CL-6B as described by Lacelle (1979). The α2–3 isomer of (*N*-acetylneuraminyl)lactose (N3L) was prepared from bovine colostrum by using the procedure of Schneir & Rafelson (1966) as described previously (Kronis & Carver, 1982). The purity of the N3L was monitored by 360-MHz ^{1}H NMR spectroscopy at 24 ± 1 °C (Kronis & Carver, 1982).

NMR Sample Preparation. Lyophilized WGA I samples were exchanged for several hours in 99.7% D_2O (Merck Sharp & Dohme) before lyophilization. This exchange was repeated 2 or more times to reduce the size of the residual HDO peak in the subsequent NMR samples (Kronis & Carver, 1982). In order to reduce autohydrolysis, N3L was exchanged in D_2O on ice. Protein solutions were obtained by dissolving D_2O-exchanged WGA I in deuterated phosphate buffer (0.1 M NaP_i–0.15 M NaCl in 99.96% D_2O, pD 6.1 ± 0.1; Kronis & Carver, 1982). A small amount of denatured protein was removed by centrifugation for 1 min at 15000*g*. The protein concentration was determined on diluted aliquots of the supernatants by using the WGA I extinction coefficient of 1.70 cm^2/mg at 277 nm and a monomer molecular weight of 17000 (Nagata & Burger, 1974; Rice & Etzler, 1974). The protein sample in deuterated buffer was split into two 1.0-mL aliquots, one of which was added to a dry, lyophilized sample of N3L of known weight (typically, 7–10 mg). The concentration of N3L was calculated by using a molecular weight of 633.6. This stock solution served as the highest concentration of total ligand ($[A]_I$) while the other sample represented a protein stock with no ligand ($[A]_T = 0$). The intermediate concentrations of ligand were made by the appropriate additions of 50 or 100 μL of one stock to an initial volume of 500 μL of the other stock. Thus, all titrations were performed at a fixed protein concentration (typically 0.1 mM), while the NMR samples differed in only the total concentration of N3L ($[A]_T$), which ranged from 0 to 15 mM. Protein and stock sample volumes of 500 μL or less were measured by using glass microliter pipets (H. E. Pedersen, Denmark).

Instrumental Conditions. Proton magnetic resonance spectroscopy was performed on a 360-MHz Nicolet spectrometer at the Toronto Biomedical NMR Centre, University of Toronto. Spectra were collected without suppression of the HDO resonance in the Fourier transform mode by using a 5-kHz sweep width, a 5-s pulse delay, 16K data points, and 16–128 scans depending upon the N3L concentration of the particular sample. A line-broadening factor of 0.1 Hz was employed after Fourier transformation of the free induction decay. Chemical shift values were measured in hertz (Hz) relative to acetone, included in each sample as an internal reference [2.225 ppm relative to internal sodium 4,4-dimethyl-4-silapentane-1-sulfonate (DSS)]. The chemical shift of acetone is independent of temperature (Atkinson et al., 1981). Samples, ranging in volume from 500 to 900 μL, were analyzed in 5-mm NMR tubes (catalogue no. 528PP, Wilmad Glass Co., Inc.). Line widths were measured at half-height (in Hz) through the use of a program on the Nicolet 1280 computer which fits the experimental points to a Lorentzian line shape. Line widths were corrected for field inhomogeneity by subtracting the line width of internal acetone (Kronis & Carver, 1982).

Measurement of the Line Widths and the Chemical Shifts of the H3a and H3e Multiplets. The NMRCAP subroutine of the Nicolet 1280 computer was used to determine the line width of the H3a and H3e resonances of NeuNAc in the presence and absence of WGA I. This interactive program allows the chemical shift, the intensity, or the line width of any one of several components of a multiplet to be adjusted. All of these parameters were varied until no further reduction could be obtained in the root mean square difference between the observed and the calculated spectra. Four lines were used to fit the H3e line shapes while three lines were used for the pseudotriplet of the H3a resonance in the N3L spectra. The observed line width was calculated as the average of the fitted lines. The chemical shift value of the H3e resonance was calculated as the average of the chemical shifts of the four lines in each spectrum. The chemical shift of the H3a resonance was determined as the average of the three lines or as the chemical shift of the middle peak of the pseudotriplet in the spectrum. The H3a chemical shift, determined in either way, was comparable. The latter method was used at high fractions of ligand bound when the other components of the multiplet were broadened and were obscured by protein resonances.

Temperature Studies. The variable temperature control of the Nicolet spectrometer was used to set the temperature for a particular titration. The actual temperature of a sample was calculated from the chemical shift of the HDO resonance. An expression that relates the ^1H chemical shift of the HDO peak from internal DSS to the temperature of the sample was determined at 220 MHz by Dr. A. A. Grey (A. A. Grey, personal communication). The corresponding equation relating the chemical shift of HDO at 360 MHz to temperature is $T = -0.254\delta + 462.6$, where δ is the chemical shift of HDO from DSS (in Hz) and T is the temperature (in °C). The Nicolet variable temperature control maintained a temperature to within ±0.3 °C during an experiment.

The titrations performed at temperatures greater than room temperature were conducted in one of two ways: (i) at a single temperature throughout or (ii) an individual set of stock solutions used to conduct five titrations at five different temperatures.

Numerical Analysis. The slopes, x and y intercepts, and correlation coefficients of the linear plots were determined by using the least-squares fitting routine of a programmable calculator (Texas Instruments, Inc.). A series of Fortran programs were written to assist in solving the Swift and Connick equations (Swift & Connick, 1962) for the apparent bound parameters, $\Delta\omega_{B_{app}}$ and $1/T_{2B_{app}}$. The expressions for both of these parameters depend on the same three variables, $\Delta\omega_B$, τ_M, and T_{2B} (see Discussion). Solutions for the equations were calculated by using input ranges of possible values for the three variables. When the calculated value of the two bound parameters were both within certain ranges or tolerance limits of the observed values, the solutions were recorded. The errors in the $\Delta\omega_{B_{app}}$ and the $1/T_{2B_{app}}$ values were estimated from the errors in the appropriate slopes used for their calculation.

Results

Upfield Shifting and Broadening of N3L Resonances upon WGA I Binding. The 360-MHz ^1H NMR spectrum of N3L in the absence of protein contains a peak, well-resolved from the other resonances, at 2.032 ppm (25 °C) corresponding to the *N*-acetyl methyl group of the terminal NeuNAc residue of this trisaccharide. Addition of WGA I causes this resonance both to shift to higher field and to broaden. As shown in Figure 1 for a titration performed at 42.0 °C, the magnitude of these two spectral perturbations depends on X_B, the fraction of the total ligand which is bound to the protein. The experiments reported in this work employed an excess of ligand over protein yet the fraction of protein sites occupied covers a range suitable for the determination of binding constants (Deranleau, 1969; see Discussion). Under these conditions, the change in chemical shift ($\Delta\delta$, in Hz), which is the difference in the observed chemical shift in the presence of WGA I (δ_{obsd}) and the chemical shift of the free peak (δ_F), is proportional to the apparent bound shift ($\Delta\omega_{B_{app}}$, in s^{-1}) and the fraction of ligand bound (X_B), as given by

$$\Delta\delta = \delta_{obsd} - \delta_F = X_B \frac{\Delta\omega_{B_{app}}}{2\pi} \quad (1)$$

Similarly, the change in the line width, measured at the half-height of the peak ($\Delta\Delta\nu$, in Hz), represents the difference in the observed line width in the presence of protein ($\Delta\nu_{obsd}$) with that in its absence ($\Delta\nu_F$). The apparent bound line width ($1/T_{2B_{app}}$, in s^{-1}) is related to $\Delta\Delta\nu$ by

$$\Delta\Delta\nu = \Delta\nu_{obsd} - \Delta\nu_F = X_B \frac{1}{\pi T_{2B_{app}}} \quad (2)$$

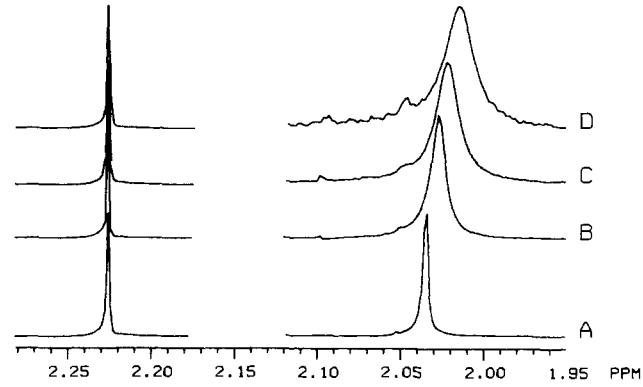

FIGURE 1: Broadening and upfield shifting of the *N*-acetyl peak of N3L by WGA I. The region of the ^1H NMR spectra of N3L containing the *N*-acetyl (2.035 ppm) and acetone (2.225 ppm) resonances are depicted in the absence (A) and the presence (B–D) of WGA I at 42.0 °C. The fraction of ligand bound, X_B, is 0% in (A), since there is no protein. The X_B values in the presence of protein are 1.0% (B), 1.6% (C), and 2.3% (D). The upfield shifting and broadening, relative to the free resonance, are proportional to X_B (see eq 1 and 2). The fractional occupancies of the WGA I sites were 73% (B), 52% (C), and 28% (D).

In the binding of a ligand, A, by a protein, P, the dissociation constant, K_D (molar), may be quantified, if $X_B \ll 1$, by using

$$[A]_T = n[P]_T(1/X_B) - K_D \quad (3)$$

where $[A]_T$ is the total ligand concentration, $[P]_T$ is the total concentration of protein monomers, n is the number of binding sites per protein monomer, and $X_B = [A]_B/[A]_T$ [see Kronis & Carver (1982)]. Equations 1 and 3 yield

$$[A]_T = n[P]_T \frac{\Delta\omega_{B_{app}}}{2\pi} \frac{1}{\Delta\delta} - K_D \quad (4)$$

In a similar manner, eq 2 and 3 yield

$$[A]_T = n[P]_T \frac{1}{\pi T_{2B_{app}}} \frac{1}{\Delta\Delta\nu} - K_D \quad (5)$$

In experiments conducted at a fixed $[P]_T$, $\Delta\delta$ and $\Delta\Delta\nu$ measurements recorded at various $[A]_T$ values may be used to construct plots, from which the values of $n\Delta\omega_{B_{app}}$ and $n(1/T_{2B_{app}})$ may be obtained (eq 4 and 5). For cases in which the resonance is shifted to higher field ($\Delta\delta < 0$), $[A]_T$ is plotted vs. $-\Delta\delta^{-1}$, and the resulting positive slope is proportional to $-n\Delta\omega_{B_{app}}$.

Temperature Dependence of $\Delta\omega_{B_{app}}$ and $1/T_{2B_{app}}$ for the N-Acetyl Resonance. In a previous room temperature study of N3L binding by WGA I at 360 MHz, the *N*-acetyl resonance did not exhibit a large change in chemical shift (Kronis & Carver, 1982). However, as the temperature was raised, the rate of chemical exchange increased, and it became possible to accurately measure $-\Delta\delta$ values. The effect of temperature on the change in chemical shift of the *N*-acetyl resonance of N3L in the presence and absence of WGA I is shown in Figure 2. At 25.4 °C (Figure 2A), $-\Delta\delta$ is small, whereas at higher temperatures (Figure 2B,C), $-\Delta\delta$ becomes larger and is quantifiable. It should be noted that the chemical shift of the free ligand varies significantly with temperature (see Figure 2), thus necessitating the recording of δ_F at each temperature in order to obtain $\Delta\delta$.

In the temperature range 31.5–47.3 °C, both $-\Delta\delta$ and $\Delta\Delta\nu$ values varied significantly over the range of ligand concentrations employed, such that the data at one temperature could be analyzed by using both eq 4 and 5. Plots of $[A]_T$ vs. the

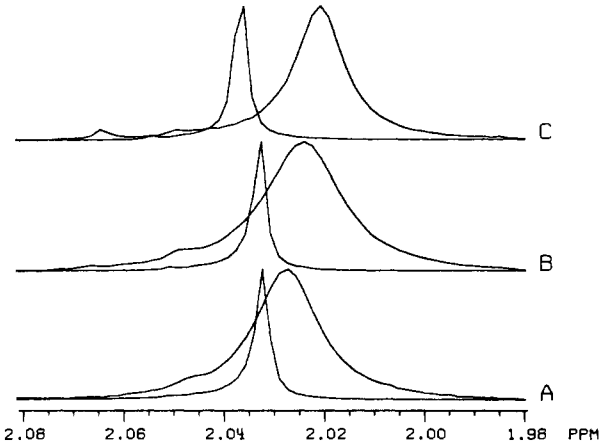

FIGURE 2: Effect of temperature on the WGA I induced shifting and broadening of the *N*-acetyl resonance of N3L. The *N*-acetyl region of the ^{1}H NMR spectrum of the ligand both with and without added protein are shown for three temperatures: 25.4 (A), 36.8 (B), and 47.3 °C (C). In each case, the sharp peak to lower field (2.03–2.04 ppm) is that of the free resonance. The broad peak to higher field represents the sample that corresponded to a comparable fraction of ligand bound (X_B = 1.6–1.7% for each temperature shown). The transition from intermediate to fast exchange is evident by the increase in the apparent shift of the resonance with temperature and by a maximum of the apparent bound line width at approximately 31 °C.

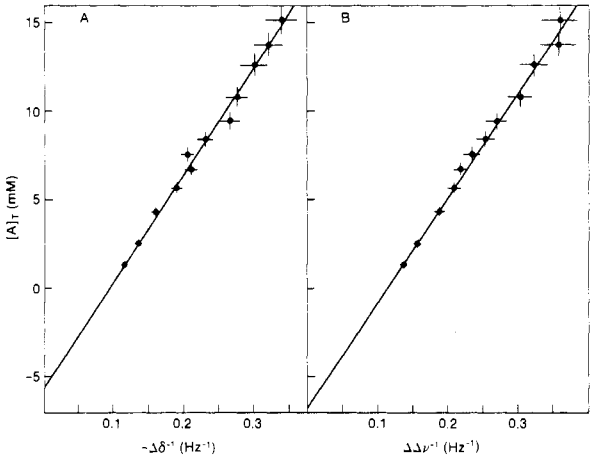

FIGURE 3: Determination of the apparent bound parameters for N3L–WGA I. Plots of total ligand concentration $[A]_T$ (millimolar) vs. the reciprocal of the upfield shift, $-\Delta\delta^{-1}$ (Hz^{-1}) (A), or vs. the reciprocal of the change in line width, $\Delta\Delta\nu^{-1}$ (Hz^{-1}) (B), are shown for the *N*-acetyl peak of N3L for a titration conducted at 42.0 °C. The slope of (A) is used to determine the apparent bound shift at that temperature, and the apparent bound line width is derived from the slope of (B), as described in the text. The *y* intercept is equal to $-K_D$ [see Kronis & Carver (1985)].

reciprocal of $-\Delta\delta$ or $\Delta\Delta\nu$ yielded straight lines at all temperatures. Typical plots, for data obtained at 47.3 °C, are shown in Figure 3A,B. The resulting values of $-n\Delta\omega_{Bapp}$ and $n(1/T_{2Bapp})$ at five temperatures are summarized in Table I. The temperature dependence of K_D is analyzed in the following paper (Kronis & Carver, 1985) for a wider range of temperatures using additional NMR data.

Temperature Dependence of $\Delta\omega_{Bapp}$ and $1/T_{2Bapp}$ for the H3a and H3e Resonances of N3L. Several other ^{1}H NMR resonances, in addition to the *N*-acetyl peak of N3L, are broadened and shifted upon binding to WGA I at 360 MHz. Most notable are the peaks corresponding to the axial and equatorial hydrogens at C-3 of the NeuNAc residue of N3L (H3a and H3e, respectively). Since these hydrogens are attached to a carbon atom on the pyranose ring that is two carbons removed from the *N*-acetylated C-5 carbon of NeuNAc, they monitor two additional environments of the N3L binding sites of WGA I. The broadening and shifting of these resonances are depicted in Figure 4 for a titration with WGA I at 47.3 °C. It is readily discernible that H3a is broadened to a greater extent than is H3e at a particular value of $[A]_T$ and hence at a particular X_B value. The H3a resonance is also shifted significantly to higher field relative to its free chemical shift under certain conditions, whereas that of H3e is perturbed to a much lesser extent (see Discussion).

Upfield shifts could be quantified for both H3e and H3a over a range of temperatures (31.5–47.3 °C). Plots of $[A]_T$ vs. $-\Delta\delta^{-1}$ allowed the determination of $-n\Delta\omega_{Bapp}$ values, the absolute values of which increased with temperature, as was observed for the *N*-acetyl peak. The temperature dependence of $-n\Delta\omega_{Bapp}$ for the H3a and H3e resonances is summarized in Table I. Line widths were obtained as described under Experimental Procedures (see Figure 5), and the changes in line widths of the H3a and H3e resonance were plotted according to eq 5 in order to calculate the corresponding $n(1/T_{2Bapp})$ values (Table I).

Table I: Temperature Dependence of the Apparent Bound Shift and Apparent Bound Line-Width Values for the *N*-Acetyl, H3a, and H3e Resonances of N3L

T (°C)	$-n\Delta\omega_{Bapp}$ (s^{-1})	c.c.[a]	$n(1/T_{2Bapp})$ (s^{-1})	c.c.[a]
		N-Acetyl		
25.4	*b*		1690	0.99
31.5	1600	0.95	2140	0.99
36.8	2800	0.99	2110	0.99
42.0	3690	0.99	1800	0.99
47.3	4160	0.99	1310	0.99
		H3a		
31.5	3180	0.96	3150	0.96
36.8	4500	0.96	4710	0.94
42.0	8080	0.96	2610	0.95
47.3	8460	0.98	2210	0.99
		H3e		
31.5	1230	0.96	930	0.98
36.8	1340	0.96	720	0.97
42.0	1440	0.98	520	0.97
47.3	1510	0.95	470	0.94

[a] The $-n\Delta\omega_{Bapp}$ and $n(1/T_{2Bapp})$ values were obtained from the slopes of plots such as those shown in parts A and B of Figure 3, respectively, using eq 4 and 5 (see Results). The correlation coefficient (c.c.) is listed following the apparent bound parameters. [b] The $-\Delta\delta$ values for the *N*-acetyl resonance at 25.4 °C were very small, and thus, no $-n\Delta\omega_{Bapp}$ value is reported.

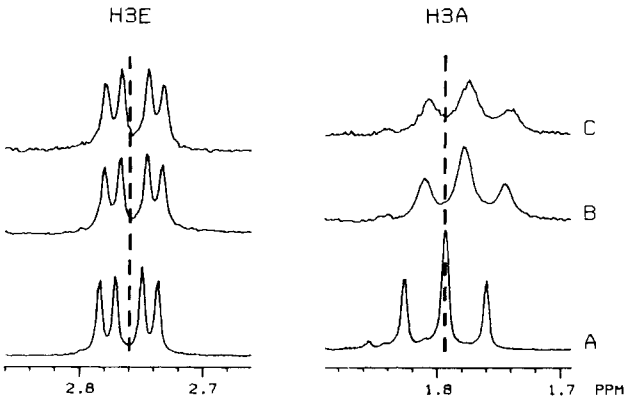

FIGURE 4: Broadening and upfield shifting of H3e and H3a peaks of N3L. The portions of the ^{1}H NMR spectra containing the resonances of the H3e (2.76 ppm) and H3a (1.79 ppm) of N3L are shown for 47.3 °C. The lower trace (A) represents the ligand in buffer alone. Addition of WGA I causes upfield shifts and broadening of these resonances, as shown in (B) for X_B = 0.9% and in (C) for X_B = 1.2%. The vertical dashed lines correspond to the free chemical shifts for the two resonances.

Table II: $\Delta\omega_B$ Solutions of the Apparent Bound Parameters for the *N*-Acetyl, H3a, and H3e Peaks for $n = 1$ and for $n = 2$[a]

			$-\Delta\omega_B$			
			$n = 1$		$n = 2$	
T (°C)	ω - tol[b] (%)	$1/T$ - tol[b] (%)	s^{-1}	ppm	s^{-1}	ppm
			N-Acetyl			
31.5	0.1	0.1	4460	1.97	2230	0.99
36.8	0.1	0.1	4400	1.95	2200	0.97
42.0	0.1	0.2	4560	2.02	2280	1.01
47.3	0.1	0.1	4570	2.02	2285	1.01
			H3a			
31.5	2	2	6180–6420	2.73–2.84	3090–3210	1.37–1.42
36.8	2	2	9260–9780	4.09–4.32	4630–4890	2.05–2.16
42.0	5	5	8560–9200	3.78–4.07	4280–4600	1.89–2.03
47.3	5	5	8640–9440	3.82–4.17	4320–4720	1.91–2.09
			H3e			
31.5	1	1	1920–1940	0.85–0.86	960–970	0.42–0.43
36.8	1	1	1710–1740	0.76–0.77	855–870	0.38
42.0	1	1	1600–1630	0.71–0.72	800–815	0.35–0.36
47.3	1	1	1630–1850	0.72–0.82	815–925	0.36–0.41

[a] The Swift–Connick equations (eq 6 and 7) were solved simultaneously at each temperature for $\Delta\omega_B$ and τ_M by using the apparent bound parameters (Table I) for the case of $n = 1$ and for $n = 2$, as described in the text. The values of τ_M obtained and their temperature dependence are reported and discussed in the following paper (Kronis & Carver, 1985). [b] The tolerance which gave one or more solutions are listed as percentages: ω - tol (%) = $|(\Delta\omega_{Bapp}^{obsd} - \Delta\omega_{Bapp}^{calcd}) \times 100|/\Delta\omega_{Bapp}^{obsd}$ and $1/T$ - tol (%) = $|(1/T_{2Bapp}^{obsd} - 1/T_{2Bapp}^{calcd}) \times 100|/(1/T_{2Bapp}^{obsd})$, where obsd = observed and calcd = calculated.

Discussion

Data Analysis Using the Swift–Connick Equations. When a nucleus, or a set of equivalent nuclei such as the *N*-acetyl methyl protons of N3L, exchanges between two (or more) chemically distinct environments such as bulk solution and a protein binding site, the change in chemical shift and the change in line width can reveal valuable information about the bound site and the rate of chemical exchange. For cases in which the fraction of ligand bound is small, Swift & Connick (1962) derived two equations for the apparent bound shift ($\Delta\omega_{Bapp}$) and the apparent bound line width ($1/T_{2Bapp}$) that both depend on three constants of the particular binding process. The Swift–Connick equations are

$$\Delta\omega_{Bapp} = \frac{\Delta\omega_B}{(1 + \tau_M/T_{2B})^2 + \tau_M^2\Delta\omega_B^2} \quad (6)$$

and

$$1/T_{2Bapp} = \frac{\tau_M/T_{2B}\,(1 + \tau_M/T_{2B}) + \tau_M^2\Delta\omega_B^2}{\tau_M[(1 + \tau_M/T_{2B})^2 + \tau_M^2\Delta\omega_B^2]} \quad (7)$$

where $\Delta\omega_B$ (in s^{-1}), the *true* bound shift, is the difference between the chemical shift of the ligand resonance at the bound site and the chemical shift of the ligand when free in solution, τ_M (in s) is the exchange lifetime and is equal to the reciprocal of the dissociation rate ($\tau_M = k_D^{-1}$), and T_{2B} (in s) is the transverse relaxation time of the bound site. Although eq 6 and 7 may be simplified under certain exchange approximations, the full expressions have been used throughout this analysis.

A program was written that varied $\Delta\omega_B$, τ_M, and T_{2B} over wide ranges of values in order to solve eq 6 and 7 iteratively for values of $\Delta\omega_{Bapp}$ and $1/T_{2Bapp}$. Solutions were recorded in which the calculated and observed values of $\Delta\omega_{Bapp}$ and $1/T_{2Bapp}$ both fell within certain tolerance limits. At the outset of these studies, it was not known whether n, the number of binding sites per WGA monomer, was equal to 1 or 2 (see below). As n is a factor in the slopes of curves used to determine the apparent bound parameters, it is present in the $\Delta\omega_{Bapp}$ and $1/T_{2Bapp}$ values listed in Table I. Thus, the Swift–Connick equations were solved for these two possible cases. In the latter instance where $n = 2$, it has been assumed

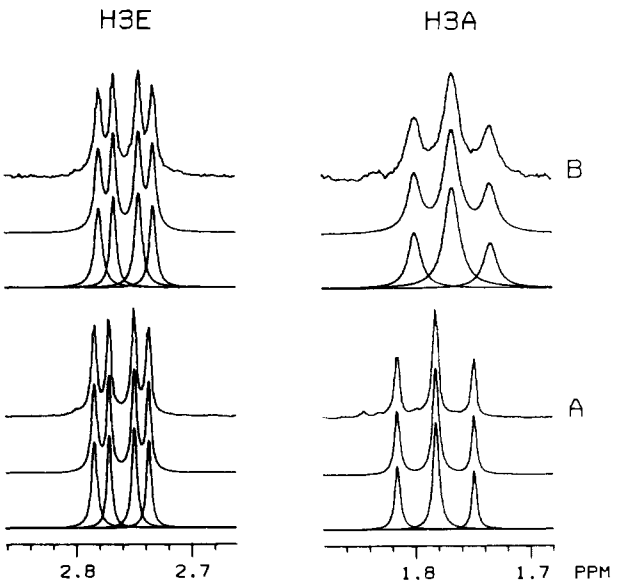

FIGURE 5: Determination of the change in line width of the H3e and H3a peaks. The H3e and H3a regions of the ^{1}H NMR spectra of N3L are shown at 47.3 °C. The traces in (A) represent the free ligand, while those in (B) correspond to a fraction of ligand bound of 1.0%. The NMRCAP program of the Nicolet 1280 computer was used to fit the experimental data with Lorentzian peaks as described in the text. The bottom of each set of three traces shows the fitted lines that gave the smallest root mean square difference with the experimental data (top trace). The middle trace is the sum of the fitted lines. Both peaks shift and broaden in the presence of WGA I, the effect being more dramatic for the H3a peak.

that both sites have identical T_{2B} and $\Delta\omega_B$ values and that τ_M is equivalent at both sites, implying that the dissociation rates from either site are the same (see below). The $\Delta\omega_B$ values obtained from the Swift–Connick equations for $n = 1$ and for $n = 2$, by using the apparent bound parameters of the *N*-acetyl, H3a and H3e resonances (Table I), are summarized in Table II.

Examination of the $\Delta\omega_B$ values listed in Table II reveals that although $-n\Delta\omega_{Bapp}$ for a given resonance showed a marked increase with increasing temperature (Table I), the $\Delta\omega_B$ obtained at each temperature is invariant. The larger scatter in the data for H3a and H3e, compared to that for the *N*-

Table III: Comparison of the $\Delta\omega_B$ (NAc) Values for NeuNAc and GlcNAc Residues Bound to WGA

ligand	NAc monitored	H_0[a] (MHz)	$-n\Delta\omega_{Bapp}$[a] (ppm)	$-n\Delta\omega_B$[a] (ppm)	$-\Delta\omega_B$[a] (ppm)	T (°C)	ref[b]
N3L	NeuNAc	360	1.84	1.98	0.99	47.3	1
GlcNAc	GlcNAc	220	2.22	2.32	1.16	36	2
$(Gn)_2Me$[c]	$GlcNAc_t$[c]	220	1.64	1.84	0.92	54	2

[a] H_0 corresponds to the field strength at which the ^1H NMR experiment was performed. $-n\Delta\omega_{Bapp}$ refers to the value obtained from the slope of $[A]_T$ vs. $-\Delta\delta^{-1}$, without assuming how many binding sites there are per monomer of WGA (n). $-n\Delta\omega_B$ was evaluated by using the full expressions of Swift & Connick (1962) in this work and by using simplified versions in Lacelle (1979) resulting from the approximation that $T_{2B} > \tau_M$. The $\Delta\omega_B$ values listed for the GlcNAc-containing ligands were assigned knowing that $n = 2$ and assuming both sites produced an identical shift (Lacelle, 1979; see Discussion also). The $\Delta\omega_B$ value listed for N3L was calculated by using $n = 2$ (see Discussion). [b] The references to these results are the following: 1, this work, 2, Lacelle (1979). [c] $(Gn)_2Me$ represents $(GlcNAc)_2\beta$1-Me. The subscript t refers to the *terminal* GlcNAc residue.

acetyl, reflects the uncertainty associated with the determination of the chemical shifts and line widths of broadened multiplets compared to singlets.

The analytical form of the temperature dependence of the apparent parameters can be predicted from the Swift–Connick equations. In Figure 6, the observed apparent parameters for the *N*-acetyl resonance ($n = 2$; see below) are plotted as squares while the predicted dependences are shown as solid lines. The values corresponding to the latter were generated by using the values obtained from the Swift–Connick solutions for $n = 2$: $\Delta\omega_B = -2250\ s^{-1}$, $T_{2B} = 1.6 \times 10^{-2}$ s, and the temperature dependence of τ_M [see Kronis & Carver (1985)]. Curves of identical shapes were obtained by using $n = 1$. At 25.4 °C, the changes in the chemical shifts of the *N*-acetyl resonance were too small for accurate quantification (Figure 2). To obtain the $\Delta\omega_{Bapp}$ value, shown as a triangle in Figure 6A, eq 7 was solved iteratively for τ_M and T_{2B} by using the $\Delta\omega_B$ and the $1/T_{2Bapp}$ values corresponding to $n = 2$.

The resulting sigmoidal curve, shown in Figure 6A, is typical of that predicted for $|\Delta\omega_{Bapp}|$ vs. $1/T$ (Dwek, 1973). Similarily, the plot of $1/T_{2Bapp}$ vs. $1/T$ (Figure 6B) shows the expected maximum at $|\tau_M\Delta\omega_B| = 1$ (Carver & Richards, 1972) resulting from the fact that in this system $|\tau_M\Delta\omega_B|$ varied with temperature from 0.3 to 2.3. It is evident from Figure 6A that only at the extreme limit of fast exchange is the *true* bound shift accurately given by $\Delta\omega_{Bapp}$; under any other conditions, $\Delta\omega_{Bapp}$ will underestimate $\Delta\omega_B$. The determination of the temperature dependence of $\Delta\omega_{Bapp}$ is clearly necessary in both establishing the appropriate exchange approximation and in obtaining reliable estimates of $\Delta\omega_B$.

αNeuNAc, like Terminal βGlcNAc, Binds to Four Tyrosine-Containing Sites on the WGA Dimer. In positioning a ligand molecule in a protein binding site, the NMR bound shift values for ligand resonances can be invaluable as long as information is available on the crystal coordinates of the protein and the protein complex [see Dwek (1973) and Perkins (1982)]. From her examination of the crystal structure of the complex of WGA II with $(GlcNAc)_2$, Wright concluded that the *N*-acetyl groups of the *terminal* GlcNAc residues have identical orientations with respect to Tyr-73[2] at the *primary* binding site and Tyr-159 at the *secondary* site (Wright, 1980b; C. S. Wright, personal communication). This identity in orientation in the crystal suggests that the solution bound shift experienced at either site due to the Tyr side chain should be the same, if the ligand orientations are the same in the crystal and solution states. Lacelle (1979) determined that $n\Delta\omega_B = -2$ ppm for the *N*-acetyl resonance of terminal GlcNAc residues bound to WGA I in solution (Table III). Since n is known to be 2 in solution for the GlcNAc-containing molecules (Nagata & Burger, 1974; Privat et al., 1974a) and the bound

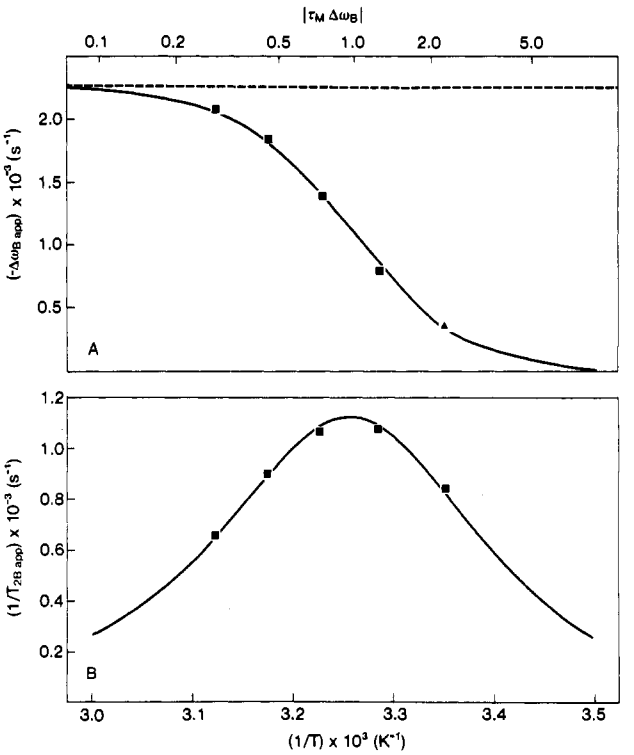

FIGURE 6: Temperature dependence of the apparent bound shift and the apparent bound line width for the *N*-acetyl peak using $n = 2$. (A) The $|\Delta\omega_{Bapp}|$ values, derived from plots such as that shown in Figure 3A, are plotted vs. the reciprocal of the temperature, $(1/T) \times 10^3$ (K^{-1}). The transition from slow through intermediate to fast exchange conditions is evident by the sigmoidal shape of the $\Delta\omega_{Bapp}$ curve with increasing temperature. The absolute values of $\tau_M\Delta\omega_B$ at various temperatures are listed on the abscissa for comparison. A dashed line represents the $-\Delta\omega_B$ value of 2250 s^{-1} (see Table II). (B) The $1/T_{2Bapp}$ values obtained from plots such as that shown in Figure 3B are plotted vs. $(1/T) \times 10^3$ (K^{-1}). The transition from slow to fast exchange is demonstrated by the increase in $1/T_{2Bapp}$ to a maximum when the absolute value of $\tau_M\Delta\omega_B$ is 1. The symbols are (■) the observed values and (▲) the $\Delta\omega_{Bapp}$ value calculated from the $1/T_{2Bapp}$ value at 25.4 °C, as described in the text.

shifts at both sites are presumably equal (see above), it follows that the aromatic rings of Tyr-73 and Tyr-159 produce −1 ppm shifts in their respective binding sites. The coordinates of the WGA II–$(GlcNAc)_2$ complex (C. S. Wright, personal communication) were used to calculate the sum of the bound shifts induced on the *N*-acetyl group of the terminal GlcNAc moiety by all of the aromatic amino acids surrounding the two sites (K. A. Kronis and J. P. Carver, unpublished results). The results are entirely consistent with the arguments given above in that both sites induced a shift of approximately −1 ppm. At the primary site this bound shift arose from Tyr-73 almost entirely, and similarly at the secondary site the bound shift arose from Tyr-159. No significant contribution from Trp-107 was found. If Tyr-73 and Tyr-159 are replaced by Trp side chains, much larger shifts are predicted than those observed. Thus, these results strongly support the interpretation of the

[2] The numbering of the amino acid residues of WGA in this paper is based upon the most recent crystallographic and peptide sequence data (Wright et al., 1984) and differs slightly from that of the earlier reports of Wright (1980a,b); for example, Tyr-73 was Tyr-71.

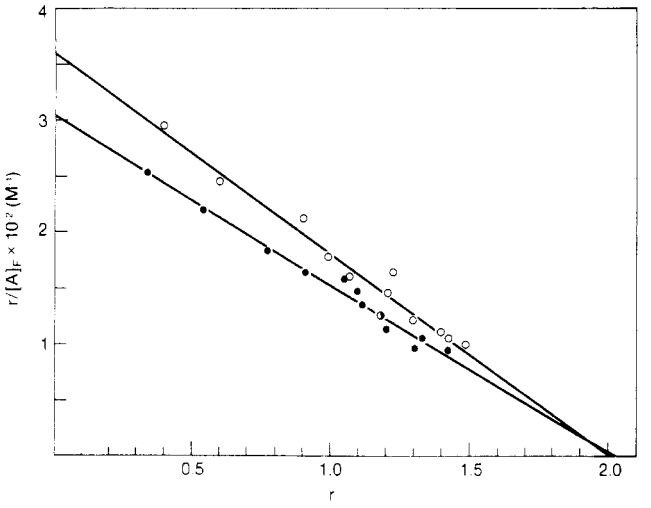

FIGURE 7: Scatchard plots of the binding data at 42.0 °C. The $\Delta\delta$ and $\Delta\Delta\nu$ values at a particular total ligand concentration were used to calculate X_B values by using the $\Delta\omega_{Bapp}$ and $1/T_{2Bapp}$ values, respectively, for the case of $n = 2$ (see Table I) using eq 1 and 2. The free concentration of ligand, $[A]_F$ (molar), was calculated by using the X_B values. The fractional occupancy of the WGA I monomers, r, was calculated as the ratio of the concentration of bound ligand, $[A]_B$, to the total monomer concentration, $[P]_T$. The least-squares fit of the plot obtained from the $\Delta\delta$ data afforded an x intercept of 2.01 and a K_D of 5.6 mM from the slope with a correlation coefficient of −0.98 (○). The fit of the plot derived from the $\Delta\Delta\nu$ values gave an x intercept of 2.02, a K_D of 6.7 mM, and a correlation coefficient of −0.99 (●).

electron density and amino acid sequencing data given by Wright et al. (1984).

From difference density maps between WGA II complexes with NeuNAc and $(GlcNAc)_2$, Wright (1980b) concluded that the orientation of the *N*-acetyl groups of NeuNAc and *terminal* GlcNAc residues are identical at the *primary* binding site. Thus, as would be expected from the results for terminal GlcNAc, the bound shift for the *N*-acetyl of N3L calculated from the coordinates at the primary site (C. S. Wright, personal communication) was found to be approximately −1 ppm, once again with almost the entire effect arising from Tyr-73 (K. A. Kronis and J. P. Carver, unpublished results). Since $n\Delta\omega_B = -2$ ppm for N3L (see Table II), there must be a contribution of −1 ppm from a site other than that at Tyr-73. It is reasonable to conclude that $n = 2$ in solution and that the second site is the Tyr-159-containing site. The identity of the aromatic amino acid in this second site is not evident from the crystallographic studies because N3L was only observed to bind at the Tyr-73 site in the crystal complex. The absence of a second binding site in the crystals is thought to arise from crystal-specific effects (C. S. Wright, personal communication; see below also).

Further support for the assumption that the *N*-acetyl-bound shifts of N3L are equivalent at the primary and secondary sites comes from Scatchard plots of the binding data. In Figure 7, representative binding data at 42.0 °C have been plotted according to Scatchard (1949). Scatchard plots were obtained from the $\Delta\omega_{Bapp}$ and $1/T_{2Bapp}$ data at all temperatures, and all were found to be linear. The linearity of these representations over the entire ranges of protein saturation and temperatures is indicative of equivalence at the two sites of the affinities, the bound shifts, and the τ_M values. The difference in the slopes of the two lines reflects the difference in the K_D values obtained from the $\Delta\delta$ and $\Delta\Delta\nu$ data and corresponds to a difference in free energy of 0.1 kcal mol^{-1} [see Kronis & Carver (1985)]. The value of n cannot be independently determined from such an analysis since it depends on the choice of $\Delta\omega_{Bapp}$ or $1/T_{2Bapp}$ used to generate X_B (see eq 1, 2, 4, and 5). When the apparent bound parameters were chosen for the case of $n = 2$, as is shown in Figure 7 for 42.0 °C, the x intercept was found to be 2.0 ± 0.05. This is an independent verification that the WGA I extinction coefficient and the monomer molecular weight used to calculate the protein concentration afford an accurate concentration of binding sites. The solution affinities at the two sites per monomer are indistinguishable by these analyses of the NMR data. Therefore, it is reasonable to assume that the interactions and thus the orientations of the ligand with respect to the protein aromatic side chains are functionally equivalent at both sites.

Since both NeuNAc and terminal GlcNAc bind to the same two subsites, the terminology of *primary* and *secondary* (Wright, 1980a,b) appears to be only relevant to the crystal complexes. We suggest instead that the primary site be referred to as the S_{BC} site since it is located at the interface of the B domain of one WGA monomer and the C domain of another (Wright, 1980a,b). The secondary site should likewise be called the S_{AD} site. Although these sites appear to interact with ligands in identical ways as detectable by affinities, and by $\Delta\omega_B$ and τ_M values for *N*-acetyl resonances, the distinction in naming them is relevant since they are not necessarily identical in architecture with respect to other amino acid side chains (C. S. Wright, personal communication).

Additional evidence in support of $n = 2$ comes from an analysis of the broadening and upfield shifting of the H3a resonance of NeuNAc. From the data reported in Table II it can be seen that $n\Delta\omega_B = -4.0$ ppm for this resonance; thus, if $n = 1$, the binding site would have to induce an upfield shift of 4 ppm. By use of the procedure outlined by Perkins (1982), the bound shifts in the vicinity of the primary binding site were calculated to be approximately −2 ppm for H3a (K. A. Kronis and J. P. Carver, unpublished observation) by using the crystal coordinates at S_{BC} (C. S. Wright, personal communication). Thus, a second site must be involved in the generation of the bound shift, and by an argument analogous to the above, we assume both sites contribute a bound shift of −2 ppm. The much smaller value of $\Delta\omega_B$ for H3e (−0.4 ppm for $n = 2$; Table II) is consistent with the orientation of the NeuNAc residue in the primary site deduced from the X-ray diffraction studies (Wright 1980a,b; K. A. Kronis and J. P. Carver, unpublished results). The values of $\Delta\omega_B$ for the *N*-acetyl methyl group and for the H3a and H3e protons obtained in these NMR studies have been used to position the NeuNAc portion of N3L in the two WGA I binding sites per monomer (K. A. Kronis and J. P. Carver, unpublished results).

There have been many studies implicating Trp residues in the interaction of WGA with its ligands (Jordan et al., 1977; Privat et al., 1974a,b; Lotan & Sharon, 1974). The NMR results reported in this work corroborate the crystallographic studies in locating a Tyr and not a Trp residue in the subsite to which both NeuNAc and terminal GlcNAc bind. The location of the Trp relative to bound GlcNAc and NeuNAc terminating ligands has also been addressed (K. A. Kronis and J. P. Carver, unpublished results).

The crystal complexes of WGA II with NeuNAc or N3L did not show electron density at S_{AD}, the Tyr-159 containing site (Wright 1980a,b). Steric crowding or electrostatic repulsion in the lattice structure of crystals of WGA could account for this observation. The possibility of steric constraints is supported by the fact that less density is observed for GlcNAc-containing molecules at this site than at S_{BC} (Wright, 1980b) and that the dimer molecules are in close

proximity at the interfaces between the A and D domains near S_{AD}; thus, acidic side chains on other WGA molecules, adjacent to the S_{AD} site in the crystal, could preferentially inhibit the binding of NeuNAc but not GlcNAc (C. S. Wright, personal communication). Clearly, this would not be a factor in the binding of sugars in solution by WGA dimers.

Since the number of binding sites for GlcNAc and NeuNAc in solution are identical, any difference in the biological consequences from the binding of one sugar vs. the other cannot be attributed to a difference in the number of sites. However, the orientation relative to the protein surface of bound molecules terminating in βGlcNAc or αNeuNAc is different. This has been shown for S_{BC} in the crystal (Wright, 1980b) and for both sites in solution (K. A. Kronis and J. P. Carver, unpublished results). This difference in orientation may lead to differential accessibility for large oligosaccharides or membrane-bound structures and thereby make important contributions to the specificity of WGA for cell surfaces.

ACKNOWLEDGMENTS

We thank Dr. Christine S. Wright for providing us with the most recent coordinates for WGA II and the complexes with NeuNAc- and GlcNAc-containing ligands. Tom Lew and Dr. Dale A. Cumming provided invaluable assistance with programming.

Registry No. NeuNAc, 131-48-6; N3L, 35890-39-2; N3L α2–3 isomer, 35890-38-1; GlcNAc, 7512-17-6; $(GlcNAc)_2$, 35061-50-8; $(GlcNAc)_3$, 38864-21-0; $(GlcNAc)_2$β1-Me, 19272-54-9; N3Ln, 81693-22-3; Tyr, 60-18-4.

REFERENCES

Adair, W. L., & Kornfeld, S. (1974) *J. Biol. Chem. 249*, 4696–4704.

Atkinson, P. H., Grey, A. A., Carver, J. P., Hakimi, J., & Ceccarini, C. (1981) *Biochemistry 20*, 3979–3986.

Bhavanandan, V. P., & Katlic, A. W. (1979) *J. Biol. Chem. 254*, 4000–4008.

Burger, M. M., & Goldberg, A. R. (1967) *Proc. Natl. Acad. Sci. U.S.A. 57*, 359–366.

Carver, J. P., & Richards, R. E. (1972) *J. Magn. Reson. 6*, 89–105.

Cuatrecasas, P. (1973) *Biochemistry 12*, 1312–1323.

Deranleau, D. A. (1969) *J. Am. Chem. Soc. 91*, 4044–4049.

Dwek, R. A. (1973) *Nuclear Magnetic Resonance (N.M.R.) in Biochemistry*, Clarendon Press, Oxford.

Goldstein, I. J., & Hayes, C. E. (1978) *Adv. Carbohydr. Chem. Biochem. 35*, 127–340.

Goldstein, I. J., Hughes, R. C., Monsigny, M., & Sharon, N. (1980) *Nature (London) 285*, 66.

Greenaway, P. J., & LeVine, D. (1973) *Nature (London), New Biol. 241*, 191–192.

Jordan, F., Bassett, E., & Redwood, W. R. (1977) *Biochem. Biophys. Res. Commun. 75*, 1015–1021.

Jordan, F., Bahr, H., Patrick, J., & Woo, P. W. K. (1981) *Arch. Biochem. Biophys. 207*, 81–86.

Kronis, K. A., & Carver, J. P. (1982) *Biochemistry 21*, 3050–3057.

Kronis, K. A., & Carver, J. P. (1985) *Biochemistry* (following paper in this issue).

Lacelle, N. (1979) Ph.D. Thesis, University of Toronto, Toronto.

Lotan, R., & Sharon, N. (1973) *Biochem. Biophys. Res. Commun. 55*, 1340–1346.

Marchesi, V. T. (1972) *Methods Enzymol. 28*, 354–356.

Nagata, Y., & Burger, M. M. (1974) *J. Biol. Chem. 249*, 3116–3122.

Perkins, S. J. (1982) in *Biological Magnetic Resonance* (Berliner, L. J., & Reuben, J., Eds.), Vol. 4, pp 193–336, Plenum Press, New York.

Peters, B. P., Ebisu, S., Goldstein, I. J., & Flashner, M. (1979) *Biochemistry 18*, 5505–5511.

Privat, J.-P., Delmotte, F., Mialonier, G., Bouchard, P., & Monsigny, M. (1974a) *Eur. J. Biochem. 47*, 5–14.

Privat, J.-P., Delmotte, F., & Monsigny, M. (1974b) *FEBS Lett. 46*, 224–228.

Rice, R. H., & Etzler, M. E. (1974) *Biochem. Biophys. Res. Commun. 59*, 414–419.

Scatchard, G. (1949) *Ann. N.Y. Acad. Sci. 51*, 660–672.

Schneir, M. L., & Rafelson, M. E., Jr. (1966) *Biochim. Biophys. Acta 130*, 1–11.

Stanley, P., & Carver, J. P. (1977) *Proc. Natl. Acad. Sci. U.S.A. 74*, 5056–5059.

Stanley, P., Sudo, T., & Carver, J. P. (1980) *J. Cell Biol. 85*, 60–69.

Swift, T. J., & Connick, R. E. (1962) *J. Chem. Phys. 37*, 307–320.

Wright, C. S. (1980a) *J. Mol. Biol. 139*, 53–60.

Wright, C. S. (1980b) *J. Mol. Biol. 141*, 267–291.

Wright, C. S., Gavilanes, F., & Peterson, D. L. (1984) *Biochemistry 23*, 280–287.